

STEADY FLOW OF A TWO-DIMENSIONAL LIQUID CURTAIN UNDER PRESSURE

Irene Moulitsas* and Georgios Georgiou**

* *The Cyprus Institute, 15 Kypranoros Street, 1061 Nicosia, Cyprus*

** *Department of Mathematics and Statistics, University of Cyprus,
P.O. Box 20537, 1678 Nicosia, Cyprus*

E-Mail: georgios@ucy.ac.cy (Corresponding Author)

ABSTRACT: We use finite elements and the full-Newton iteration method to solve the steady, two-dimensional flow of a Newtonian planar film issuing from a slit under a pressure difference, in the presence of gravity and surface tension. The simulated film shapes agree with available experimental data within the range of the experimental error. The numerical calculations show that the shape of the film depends strongly on the imposed pressure difference, inertia and gravity, and is rather insensitive to surface tension.

Keywords: planar film, extrudate swell, finite elements, gravity, surface tension

1. INTRODUCTION

The extrusion of two-dimensional or annular sheets is important in many industrial applications, such as coating processes, film blowing, atomization, and paper manufacturing, and has been the subject of experimental, theoretical, and numerical studies (see De Luca (1999), Roche et al. (2006), Clanet (2007) and references therein). Finnicum, Weinstein and Ruschak (1993) studied theoretically and experimentally the effect of applied pressure on a two-dimensional liquid curtain issuing from a slot and falling under the influence of gravity. They obtained an approximate equation for the location of the curtain which, in addition to gravity and the applied pressure, also takes into account the surface tension. Their theoretical model is based on the assumption that the thickness of the curtain varies very slowly as it falls vertically, i.e., it is nearly one-dimensional. Their theoretical predictions involving an experimentally determined constant are in agreement with their experimental results.

The objectives of the present work are: (a) to solve numerically the steady, two-dimensional flow of a planar Newtonian curtain issuing from a slit and under a pressure difference, taking into account gravity and surface tension effects; and (b) to make comparisons with the experimental film shapes provided by Finnicum, Weinstein and Ruschak (1993). The finite element method with the full-Newton iteration technique for the calculation of the unknown positions of the two free surfaces of the film is well established and is

described elsewhere (Georgiou, Papanastasiou and Wilkes, 1988; Housiadas, Georgiou and Tsamopoulos, 2000; Georgiou, 2003).

In Section 2, the governing equations and the boundary conditions of the flow are presented, and an outline of the finite element method used in the simulations is given. In Section 3, the numerical results are presented and discussed. The predicted shapes of the film agree only qualitatively with the experimental ones provided by Finnicum, Weinstein and Ruschak (1993). Some explanations for the differences between simulations and experiments are provided. Our conclusions are summarized in Section 4.

2. GOVERNING EQUATIONS

The geometry of the flow is depicted in Fig. 1a. The flow is assumed to be steady, incompressible, isothermal, and Newtonian. The governing equations are nondimensionalized by scaling lengths by the slit width W , the velocity vector, \mathbf{v} , by the average velocity U in the slit, and the pressure, p , and the stress tensor, $\boldsymbol{\tau}$, by $\mu U/W$, where μ is the constant viscosity. The resulting dimensionless forms of the continuity and momentum equations are:

$$\nabla \cdot \mathbf{v} = 0 \quad (1)$$

and

$$\text{Re } \mathbf{v} \cdot \nabla \mathbf{v} = -\nabla p + \nabla \cdot \boldsymbol{\tau} + St \mathbf{i} \quad (2)$$

where

$$Re \equiv \frac{\rho U W}{\mu} \quad (3)$$

and

$$St \equiv \frac{\rho g W^2}{\mu U} \quad (4)$$

are the Reynolds and Stokes numbers, respectively, ρ is the density, g is the gravitational acceleration, and \mathbf{i} denotes the unit vector in the x -direction (Fig. 1a).

The boundary conditions of the flow are shown in Fig. 1b. At the inlet plane, taken at a distance L_1 upstream the die exit, the flow is assumed to be fully developed, i.e., v_x is given by the standard Poiseuille profile $6(y - y^2)$ and $v_y=0$. Along the solid walls, both the velocity components vanish (i.e., no slip is assumed). At the outlet plane, taken at a distance L_2 downstream from the die exit, the flow is assumed to be approximately uniform, and, thus,

$$T_{xx} = -p + \tau_{xx} = 0 \quad \text{and} \quad v_y = 0 \quad (5)$$

where T_{xx} and τ_{xx} are respectively the total and viscous normal stress components. (The subscript xx denotes here the xx -component of a tensor.) Of course, the above set of boundary conditions is not valid when the film is deflected, i.e., when p_A

is nonzero. However, they lead to satisfactory results up to a certain fraction of the length L_2 , provided that the latter is sufficiently long. Other combinations of boundary conditions at the outlet plane have also been used and are discussed below.

There remain the boundary conditions along the two free surfaces. It is assumed that the external pressure p_A is applied on the lower free surface (Fig. 1b). The kinematic condition on the two free surfaces,

$$\mathbf{n} \cdot \mathbf{v} = 0 \quad (6)$$

where \mathbf{n} is the unit normal vector pointing outwards from a free surface, provides the two additional equations needed for the calculation of the unknown positions h_1 and h_2 of the lower and upper free surfaces, respectively (Georgiou, Papanastasiou and Wilkes, 1988; Housiadas, Georgiou and Tsamopoulos, 2000; Georgiou, 2003).

A momentum balance on the upper free surface requires the shear stress to vanish and the normal stress in the liquid to balance any capillary pressure,

$$\mathbf{n} \cdot \mathbf{T} = -\frac{2H}{Ca} \mathbf{n} \quad (7)$$

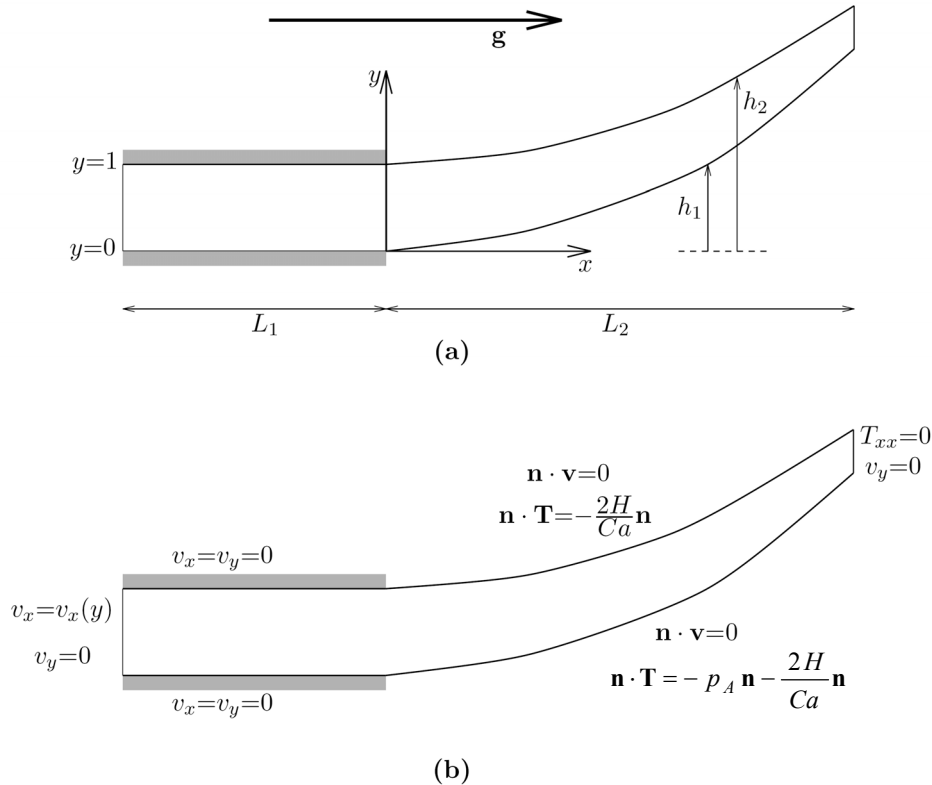


Fig. 1 Geometry and boundary conditions of the flow of a two-dimensional curtain issuing from a slit under pressure.

In the above equation,

$$\mathbf{T} = -p\mathbf{I} + \boldsymbol{\tau} = -p\mathbf{I} + \nabla\mathbf{v} + (\nabla\mathbf{v})^T \quad (8)$$

is the total stress tensor, \mathbf{I} is the unit tensor, Ca is the capillary number, defined by

$$Ca \equiv \frac{\mu U}{\sigma} \quad (9)$$

where σ denotes the surface tension, and $2H$ is the mean curvature of the free surface, given by

$$-2H = \frac{h''}{(1+h'^2)^{3/2}} \quad (10)$$

where h' and h'' are respectively the first and second derivative of $h(x)$ with respect to x . Similar expressions hold for the lower free surface, where, however, the external pressure p_A must be taken into account, i.e.,

$$\mathbf{n} \cdot \mathbf{T} = -p_A \mathbf{n} - \frac{2H}{Ca} \mathbf{n} \quad (11)$$

The above governing equations and boundary conditions have been solved using finite elements. The Newton method has been employed in order to solve the resulting nonlinear system of the discretized equations. In other words, the five unknowns, v_x , v_y , p , h_1 , and h_2 , are calculated simultaneously. The numerical method is discussed elsewhere (Georgiou, Papanastasiou and Wilkes, 1988; Housiadas, Georgiou and Tsamopoulos, 2000; Georgiou, 2003).

Table 1 Data for some of the meshes used in the present work.

Mesh	L_2	N_x	N_y	Number of elements	Number of unknowns
1	1600	317	10	3170	31311
2	1000	774	10	7740	76554
3	1000	1359	10	13590	134469
4	600	1359	10	13590	134469

We used meshes of different lengths and degrees of refinement to investigate the robustness of the boundary condition at the outflow plane. In Table 1, useful data for some of the meshes used in the calculations are tabulated. N_x and N_y denote the numbers of elements in the x - and y -direction, respectively. All meshes were graded, with the element dimensions becoming progressively smaller towards the exit plane and the walls. As discussed in Section 3, the method diverges above a critical value of p_A which depends on the Reynolds, Stokes and capillary numbers. In an

attempt to extend the numerical calculations to higher values of p_A , we also tried to apply the so-called free outflow boundary condition (Malamataris and Papanastasiou, 1991; Papanastasiou, Malamataris and Ellwood, 1992). Two different combinations have been considered. In the first one, both the stress components at the outflow plane were free:

$$T_{xx} = -p + 2 \frac{\partial v_x}{\partial x} \quad \text{and} \quad T_{xy} = \frac{\partial v_x}{\partial y} + \frac{\partial v_y}{\partial x} \quad (12)$$

In the second combination only T_{xy} was free, that is

$$T_{xx} = 0 \quad \text{and} \quad T_{xy} = \frac{\partial v_x}{\partial y} + \frac{\partial v_y}{\partial x} \quad (13)$$

The results obtained in both cases are essentially the same as those obtained with boundary conditions (5), except in a small region near $x=L_2$.

3. RESULTS AND DISCUSSION

The values of all the dimensionless flow parameters in the two experiments of Finnicum, Weinstein and Ruschak (1993) are tabulated in Table 2. We first obtained results for the case of zero applied pressure ($p_A=0$), in order to get some initial information about the behavior of the solution and test the convergence of the numerical solution with mesh refinement. When $p_A=0$, the flow is, of course, reduced to the planar extrudate-swell problem and the two free surfaces are symmetric about the midplane of the slit. L_1 was taken equal to 5, in all runs. In Fig. 2, we plot the calculated upper free surfaces with Meshes 1 and 2 for (a) $Re=St=0$, (b) $Re=12.1$, $St=0$, and (c) $Re=12.1$, $St=0.063$, with zero surface tension ($Ca=\infty$). A zoom of Fig. 2 near the exit is provided in Fig. 3. It is clear that the predictions with the two meshes are essentially the same. Note also that in case (a) the elevation of the upper free surface far downstream is 1.093. This value corresponds to an extrudate-swell ratio of 1.186 which agrees well with previous studies (Georgiou and Boudouvis, 1999), and indicates that the mesh refinement near the die exit is satisfactory. The effect of the gravitational force is important and results in considerable reduction of the film thickness, in agreement with previous work (Georgiou, Papanastasiou and Wilkes, 1988). The calculated upper free surfaces for the dimensionless numbers corresponding to the two experiments of Finnicum, Weinstein and Ruschak (1993) are plotted in Fig. 4. Again the applied external pressure is taken to be zero.

Table 2 Values of the dimensionless parameters in the two experiments of Finnicum, Weinstein and Ruschak (1993).

Experiment	Re	St	Ca	$p_A \times 10^3$
1	12.1	0.063	0.331	2.21
				6.88
				18.7
2	5.97	0.127	0.165	2.97
				8.89
				18.8

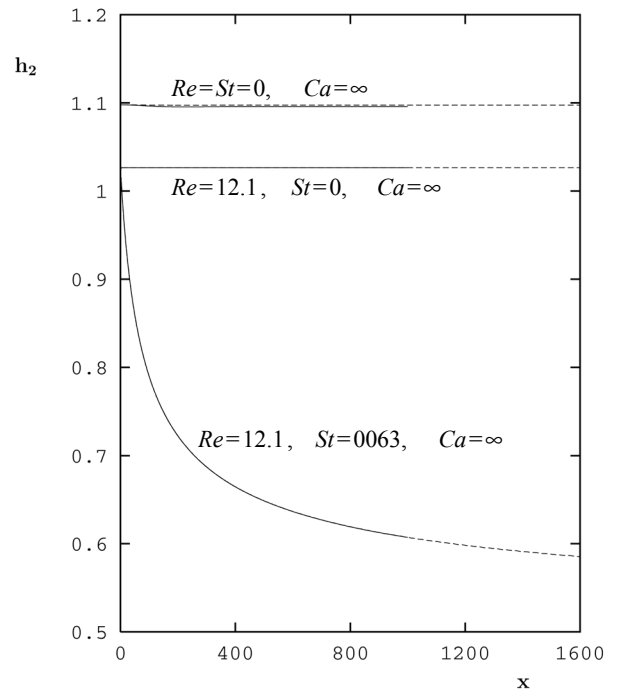


Fig. 2 Effect of the Reynolds and Stokes numbers on the upper free surface with $L_2=1000$ (solid line) and 1600 (dashed line); no pressure difference.

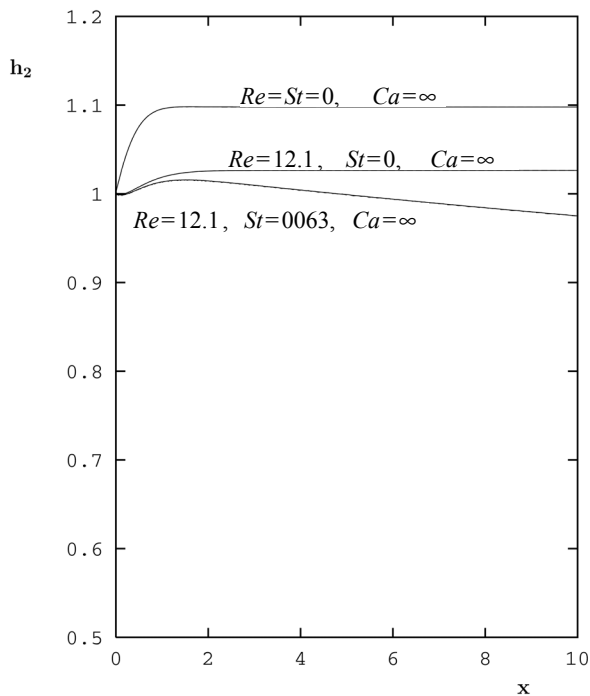


Fig. 3 Zoom of Fig. 2 near the die exit.

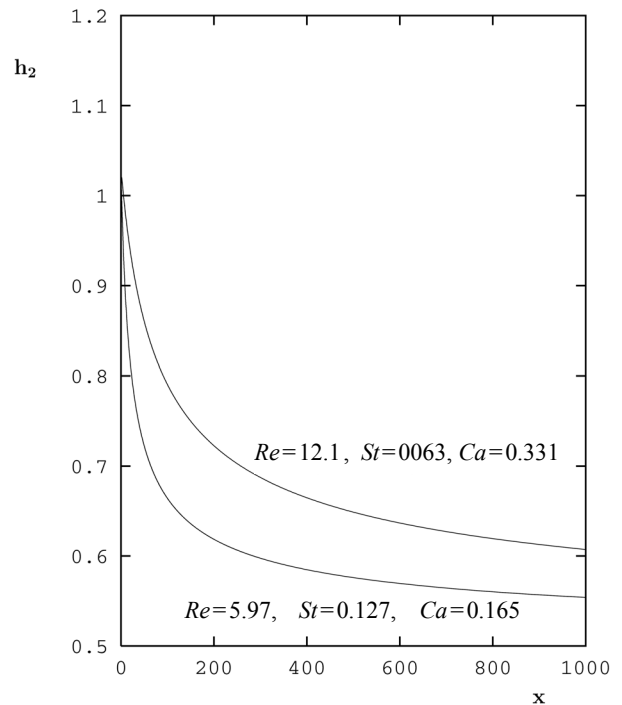


Fig. 4 Calculated upper free surfaces in the absence of pressure difference for two sets of experiments by Finnicum, Weinstein and Ruschak (1993).

In Fig. 5, we plot the film shapes calculated with Mesh 1 for different values of p_A and with the remaining parameters equal to those of the first experiment of Finnicum, Weinstein and Ruschak (1993). Beyond a critical distance from the die exit, which is reduced as p_A is increased, the calculated free surfaces are tainted by oscillations at rather low values of p_A , and the method diverges at higher applied pressures. The oscillations are entirely due to the poor mesh refinement and are eliminated by using the more refined and shorter Mesh 3, as shown in Fig. 6. Nevertheless, it has not been possible to extend the calculations to values of p_A greater than 0.01. As explained below, the divergence of the method when the liquid film is highly curved is due to the limitations of the spine technique used in constructing the finite element mesh rather than inadequate mesh refinement. Comparison of Figs. 5 and 6 shows that, apart from the oscillations, the predicted shapes of the liquid curtain with Meshes 1 and 3 ($L_2=1600$ and 1000, respectively) are the same. An interesting observation is that the film thickness varies significantly in the direction of the flow, in contrast to the assumption made in the analysis of Finnicum, Weinstein and Ruschak (1993). Our calculations with different values of Ca showed that, for the Reynolds and Stokes numbers of interest, the effect of surface tension on the shape of the film is negligible.

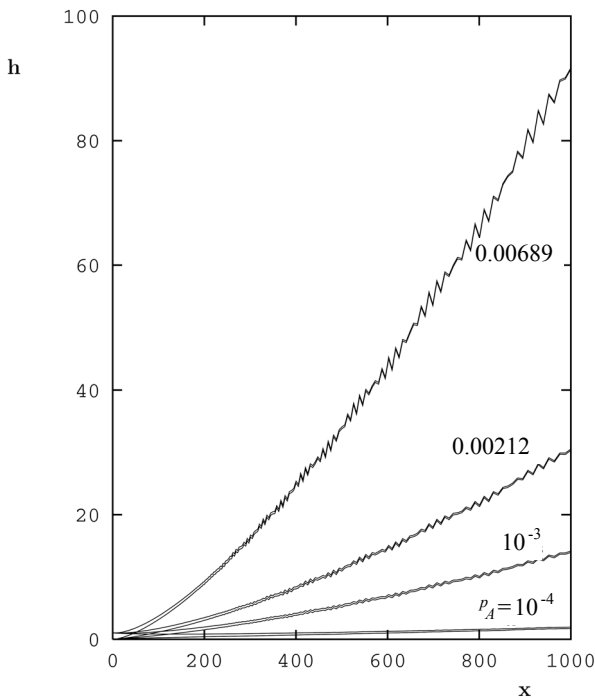


Fig. 5 Films obtained for different values of p_A with Mesh 1; $Re=12.1$, $St=0.063$ and $Ca=0.331$.

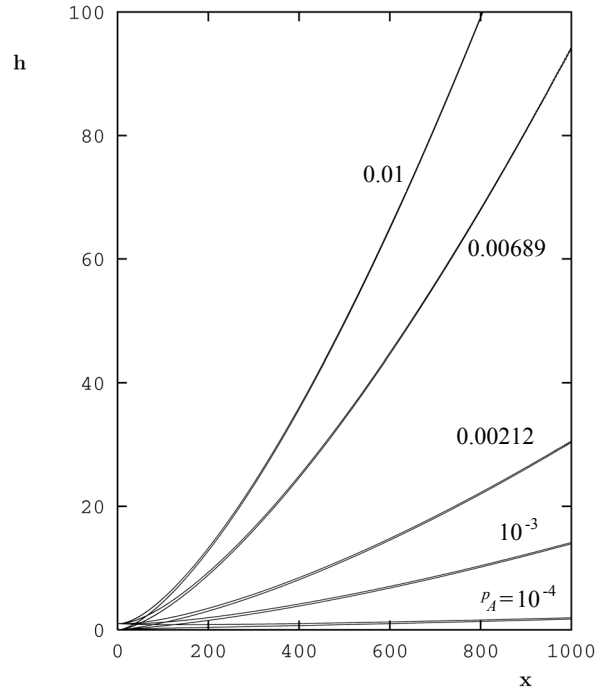


Fig. 6 Films obtained for different values of p_A with Mesh 3; $Re=12.1$, $St=0.063$ and $Ca=0.331$.

Finally, in Figs. 7 and 8, we compare the numerically predicted film shapes with the experimental data of Finnicum, Weinstein and Ruschak (1993). There is only qualitative agreement between simulation and experiment. The deviations of the film from the x -axis seem to be underestimated in the calculations and the discrepancies from the experiment increase with p_A . However, the observed differences are within the range of the experimental error. As pointed out by Finnicum, Weinstein and Ruschak (1993), the measurement precision of the micromanometers used in the experiments is ± 25 dyne/cm², whereas the highest experimental pressure difference is 7.6 dyne/cm².

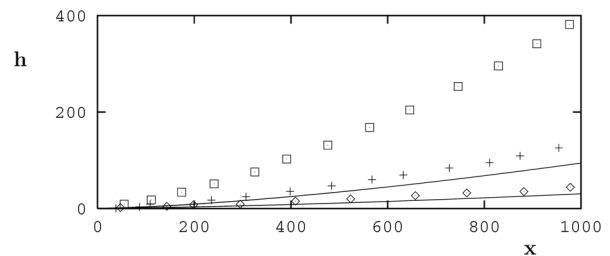


Fig. 7 Comparisons with experimental data of Finnicum, Weinstein and Ruschak (1993) for $Re=12.1$, $St=0.063$, $Ca=0.331$ and $p_A=0.00212$ (\diamond) and 0.00689 ($+$). The experimental data for $p_A=0.0187$ (\square) are also shown.

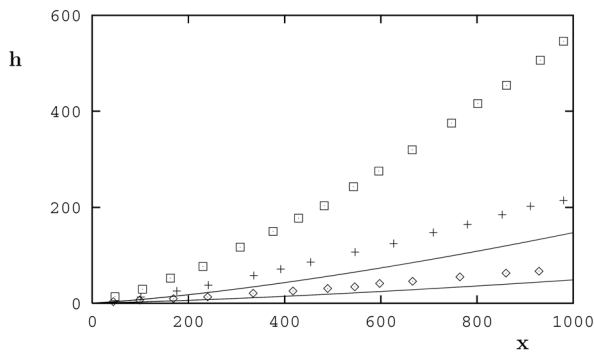


Fig. 8 Comparisons with experimental data of Finnicum, Weinstein and Ruschak (1993) for $Re=5.97$, $St=0.127$, $Ca=0.165$ and $p_A=0.00297$ (\diamond) and 0.0089 ($+$). The experimental data for $p_A=0.0188$ (\square) are also shown.

The divergence of the method at high values of p_A may be attributed to the distortion of the finite element mesh. Note that the mesh is updated at each iteration of the Newton method according to the newly found positions of the lower and upper free surfaces, using the spine technique (Georgiou, Papanastasiou and Wilkes, 1988; Georgiou, 2003). The two sides of the rectangular finite elements are vertical, and thus the more the liquid curtain deviates from the x -axis, the more distorted the elements become. A different approach, such as the quasi-elliptic mesh-generating scheme for moving boundary and free-surface problems developed by Dimakopoulos and Tsamopoulos (2007), must, therefore, be employed in order to extend the range of convergence of the method.

4. CONCLUSIONS

We have used finite elements to solve the steady, two-dimensional flow of a Newtonian planar film, under a pressure difference, gravity and surface tension. The simulated film shapes agree qualitatively with experiments. However, the differences between simulations and experiments are within the range of the experimental error. Our simulations reveal that, in the range of Reynolds and Stokes numbers examined, the film thickness is reduced significantly in the direction of the flow and the effect of the surface tension on the shape of the film is negligible. The proposed method is not applicable for high values of the applied pressure difference, in which case special meshing techniques are required for the calculation of the position of the film which deviates significantly from the plane of the slit.

REFERENCES

1. Clanet C (2007). Waterbells and liquid sheets. *Ann. Rev. Fluid Mech.* 39:469–496.
2. De Luca L (1999). Experimental investigation of the global instability of plane sheet flows. *J. Fluid Mech.* 399:355–376.
3. Dimakopoulos Y, Tsamopoulos J (2007). Transient displacement of Newtonian and viscoelastic liquids by air in complex tubes. *J. Non-Newtonian Fluid Mech.* 142:162–182.
4. Finnicum DS, Weinstein SJ, Ruschak KJ (1993). The effect of applied pressure on the shape of a two-dimensional liquid curtain falling under the influence of gravity. *J. Fluid Mech.* 255:647–665.
5. Georgiou G (2003). Annular liquid jets at high Reynolds numbers. *Int. J. Numer. Methods Fluids* 42:117–130.
6. Georgiou GC, Boudouvis A (1999). Converged solutions of the Newtonian extrudate swell problem. *Int. J. Numer. Methods Fluids* 29:363–371.
7. Georgiou GC, Papanastasiou TC, Wilkes JO (1988). Laminar jets at high Reynolds and high surface tension. *AIChE J.* 24:1559–1562.
8. Housiadas K, Georgiou G, Tsamopoulos J (2000). The steady annular extrusion of a Newtonian liquid under gravity and surface tension. *Int. J. Numer. Methods Fluids* 33:1099–1119.
9. Malamataris N, Papanastasiou TC (1991). Unsteady free surface flows on truncated domains. *Ind. Eng. Chem. Res.* 30:2211–2219.
10. Papanastasiou TC, Malamataris N, Ellwood K (1992). A new outflow boundary condition. *Int. J. Numer. Methods Fluids* 14:587–608.
11. Roche JS, Le Grand N, Brunet P, Lebon L, Lemat L (2006). Perturbations of a liquid curtain near break-up: wakes and free edges. *Phys. Fluids* 18:082101.